

# Automated Detection of Sublethal Pesticide Exposure in Honey Bees Using Temporal Attention Networks

Ethan Liang

*The Harker School, San Jose, CA, 95129, USA*

---

## ARTICLE INFO

---

### Keywords:

Honey Bee Behavioral Monitoring  
Acoustic Biosensing  
Pesticide Exposure Detection  
Multimodal Deep Learning  
Weather-Contextualized Modeling

---

## ABSTRACT

Pesticide contamination threatens ecosystems, yet traditional monitoring through soil and water sampling cannot capture spatial exposure heterogeneity or provide real-time alerts. Honey bee colonies foraging across 7 km<sup>2</sup> daily offer distributed biosensing capacity, but current detection methods require weeks of laboratory analysis or rely on subjective manual observation. Recent automated tracking demonstrates that pesticide exposure alters foraging patterns, yet these approaches analyze treatment-control comparisons rather than predicting unknown contamination. Acoustic monitoring encodes exposure information but uses shallow machine learning that cannot capture temporal dependencies. Critically, no prior work addresses weather as a confounding variable despite evidence that meteorological conditions dramatically influence both foraging and acoustics, potentially masking or mimicking pesticide effects. We introduce the Weather-Contextualized Multimodal Network (WCM-Net), integrating foraging behavior and colony acoustics with explicit weather control for pesticide exposure detection. Weather-contextualized gating learns which behavioral features maintain predictive power despite environmental variation, while cross-modal attention captures synergistic foraging-acoustic relationships. Evaluated on 433 individually tagged bees across six colonies exposed to field-realistic pesticide concentrations over 30 days, WCM-Net achieved reliable detection within three days with an AUC of 0.736±0.061, sustaining a mean AUC of 0.805±0.036 and a peak AUC of 0.829. Weather contextualization contributed 0.078 AUC and cross-modal fusion added 0.056 AUC, outperforming audio-only and foraging-only approaches by 0.103–0.123 AUC and achieving threshold detection 7–11 days earlier than traditional machine learning baselines. Feature attribution identified temporal behavioral rhythms as the most sensitive early indicators, aligning with circadian disruption mechanisms. This automated system enables beekeepers to relocate hives from contaminated sites and provides regulatory agencies with evidence for compliance monitoring and contamination source identification. Additionally, the weather-contextualized multimodality fusion could be generalized to behavioral monitoring under variable environmental conditions.

---

## 1. Introduction

Pesticide contamination in agricultural landscapes poses significant ecosystem risks, yet effective monitoring remains challenging due to the spatial and temporal heterogeneity of exposure (Han, Tian, Li, Yao, Yao, Zhang and Wu, 2025). Traditional environmental monitoring relies on soil and water sampling at fixed locations, which is resource-intensive, spatially limited, and provides only periodic snapshots of contamination status. These methods often fail to capture pesticide drift events, cumulative low-level exposure, or contamination in areas distant from application sites (Olawade, Wada, Ige, Egbewole, Olojo and Oladapo, 2024). Biological indicators offer complementary

advantages for environmental monitoring: they integrate exposure across time and space, respond to biologically relevant concentration ranges, and provide ecologically meaningful assessments of contamination impacts. Among biological indicators, honey bees are particularly valuable due to their extensive foraging range (7 km<sup>2</sup> per colony), continuous environmental sampling through daily foraging trips, and high sensitivity to neurotoxic compounds (Papa, Pellecchia, Capitani and Negri, 2025).

Current pesticide exposure monitoring in honey bees relies on three approaches with significant limitations for real-time environmental detection. Chemical residue analysis quantifies pesticide concentrations in honey, pollen, and bee tissues but requires destructive sampling, expensive laboratory processing, and weeks of analysis time (Smith,

---

\*Corresponding author

✉ [e1cago2020@gmail.com](mailto:e1cago2020@gmail.com) (E. Liang)

ORCID(s): 0009-0004-6302-1412 (E. Liang)

Vorce, Holler, Shimomura, Maglilo, Jacobs and Huestis, 2007). Molecular biomarkers, including gene expression profiling and enzyme activity assays, offer increased sensitivity to sublethal exposure but require destructive sampling and delayed laboratory analysis (Shen, Qi, Zeng, Li, Liu, Zhu and Cao, 2025). Manual behavioral observation relies on trained observers conducting assessments on fixed schedules, limiting scalability and objectivity in identifying exposure effects (Polders, Van Haperen and Brijs, 2018). These constraints motivate automated behavioral monitoring systems that can detect pesticide exposure non-invasively, continuously, and at scale.

Recent advances in computer vision and radio frequency identification (RFID) systems enable continuous tracking of individual bee flight activity. Studies using these high-resolution behavioral datasets have demonstrated that pesticide exposure causes measurable foraging behavioral changes through statistical methods, such as ANOVA and GLMMs, applied to treatment-control comparisons. However, whether behavioral patterns can predict unknown pesticide exposure remains largely unexplored (Robb, Regina and Baker, 2017). This predictive capability is essential for real-world environmental monitoring, where exposure events are unknown and must be detected proactively rather than confirmed post-hoc through controlled experiments.

Recent studies have demonstrated successful detection of pesticide exposure and air pollutants from hive acoustics alone, validating the feasibility of sound-based biosensing (Mustafa, Mohaghegh, Ardekani and Sarrafzadeh, 2025). However, these approaches rely on shallow machine learning architectures that cannot capture complex temporal dependencies in acoustic patterns. Furthermore, while observational studies have also confirmed that meteorological conditions significantly influence both foraging behavior and colony acoustics, no prior work incorporates weather as an explicit control variable in predictive frameworks (Ngo, Rustia, Yang and Lin, 2021; Goerlitz, 2018; Jhawar, Davidson, Weidenmüller, Wild, Dormagen, Landgraf and Smith, 2023). These

acoustic-based methods ignore a fundamental challenge: weather-driven behavioral variation can mask or mimic pesticide-induced changes, causing false positives during storms or false negatives during heat stress. Without weather contextualization, detection systems cannot distinguish pesticide effects from normal environmental adaptation.

We address these limitations through three contributions. First, we introduce WCM-Net, the first automated pesticide detection system integrating foraging behavior and colony acoustics with explicit weather control. This architectural principle generalizes beyond pesticide monitoring to behavioral surveillance systems operating under variable environmental conditions, including wildlife tracking and precision agriculture. Second, in WCM-Net, weather-contextualized gating learns which behavioral patterns indicate pesticide exposure across varying conditions versus normal climate responses, while cross-modal attention captures synergistic foraging-acoustic relationships that unimodal approaches miss. Third, we identified that temporal behavioral rhythms such as first departure hour and last return hour provide the most sensitive early indicators of pesticide exposure through feature attribution analysis. These patterns align with established neurotoxicology mechanisms, including circadian disruption preceding motor impairment (Ahsan, Wu, Lin, Ji and Wang, 2025), validating biologically meaningful learning and providing actionable guidance for field deployment prioritization.

## 2. Related Work

### 2.1. Pesticide Effects on Bee Foraging Behavior

Sublethal pesticide exposure disrupts multiple behavioral systems in honey bees even at concentrations below those causing acute mortality. Neonicotinoids, organophosphates, and pyrethroids impair spatial memory, navigation, and circadian regulation through different neural mechanisms (Cabirol and Haase, 2019; Robb et al., 2017; Soderlund, 2010). O'Reilly et al. demonstrated that dimethoate reduced colony departures by 67%, while lambda-cyhalothrin reduced

pollen returns by 62% (O'Reilly and Stanley, 2023). Barascou et al. found that sublethal doses of sulfoxaflor at 16 and 60 ng decreased daily flight activity by 24–33% in a dose-dependent manner (Barascou, Requier, Sené, Crauser, Le Conte and Alaux, 2022). Colin et al. demonstrated that trace imidacloprid exposure during the larval stage reduced lifetime foraging flights by 28% (Colin, Meikle, Wu and Barron, 2019). These behavioral disruptions establish that foraging activity patterns serve as sensitive indicators of pesticide exposure.

## 2.2. Acoustic Environmental Monitoring

Recent studies have demonstrated that beehive acoustics can serve as biological indicators of environmental stressors. Di et al. and Yu et al. showed that beehive sounds can detect environmental pollution and specific air pollutants using K-Nearest Neighbors (KNN), Random Forest (RF), and Support Vector Machines (SVM) (Di, Zhu, Hu, Sharif, Yu and Liu, 2025; Yu, Huang, Sharif, Di and Liu, 2025; Yu, Huang, Sharif, Jiang, Di and Liu, 2023). Zhao et al. used an SVM with Mel-frequency cepstral coefficients (MFCCs) to classify pollutant exposure from acoustic data (Zhao, Deng, Zhang, Di, Jiang and Li, 2021). Otesbelgue et al. employed Hidden Markov Models (HMM) to detect sublethal pesticide exposure to chlorpyrifos in stingless bees through sound analysis alone (Otesbelgue, Orth, Fong, Fassbinder-Orth, Blochtein and Pereira, 2025). While these studies established the feasibility of acoustic-based detection using traditional machine learning approaches, the potential of deep learning architectures, particularly attention-based models, to capture complex temporal patterns in pesticide-induced acoustic disruptions has not been investigated.

## 2.3. Weather Confounds in Behavior

Weather represents a critical confounding variable in behavioral analysis, as temperature, humidity, and wind significantly influence both foraging activity and acoustic signatures. Vincze et al. reported that bees typically forage optimally between 20–30 °C, with activity decreasing at wind speeds above 1.6–6.7 m/s, and that foraging activity is negatively correlated with humidity (Vincze, Lelelőssy, Zajácz and Mészáros,

2024). For acoustic patterns, Saha et al. found that wingbeat frequencies, the primary acoustic signal produced by flying bees, increase with temperature at approximately 2.02 Hz/°C (Saha, Genoud, Park and Thomas, 2024). These observational findings establish that any behavioral and acoustic detection system must account for weather-related variations to isolate pesticide-specific patterns from environmental confounds.

## 2.4. Bee Tracking Technologies

Multiple tracking approaches have been developed to monitor individual bee behavior at scale. Colin et al. used RFID technology with separated traffic tunnels to track individual honey bee foraging performance in full-strength field colonies across different environments and seasons (Colin, Warren, Quarrell, Allen and Barron, 2022). Wild et al. introduced binary-coded visual markers approximately 2 mm in diameter, enabling deep convolutional neural networks to identify individual bees in dense hive environments (Wild, Sixt and Landgraf, 2018). Boenisch et al. and Gernat et al. employed similar marker-based systems with automated image analysis for long-term behavioral tracking (Boenisch, Wild, Dormagen et al., 2021; Gernat, Rao, Middendorf et al., 2022). The BeesBook project uses uniquely coded markers and high-resolution cameras to track all individuals over their entire lifespan, enabling reconstruction of complete social networks (Dormagen and Wild, 2021). Our study employs computer vision with visual markers as a scalable and affordable alternative to RFID systems for tracking individual foraging activities.

## 3. Experimental Design and Setup

We collected data from the bee colonies housed in standardized 10-frame Langstroth hives containing  $48,500 \pm 4,200$  workers (mean  $\pm$  SD, assessed by standardized frame coverage method following Delaplane, Van Der Steen and Guzman-Novoa (2013)) in San Jose, California (37.33°N, 121.89°W) in 2024 and 2025. We designed three treatment groups to evaluate pesticide impacts on foraging behavior: (1)

Control - 50% sucrose solution, (2) Imidacloprid exposure - 10 ppb in 50% sucrose solution, and (3) Bifenthrin exposure - 10 ppb in 50% sucrose solution. Pesticide concentrations were selected to represent field-realistic sublethal exposure levels based on residue studies in agricultural environments (Sanchez-Bayo and Goka, 2014; Woodcock, Bullock, Shore, Heard, Pereira, Redhead and Pywell, 2017). Pesticide solutions were prepared from commercial formulations: imidacloprid from BioAdvanced Tree and Shrub Protect and Feed (1.47% concentrate) and bifenthrin from Sevin Garden Insect Killer Ready to Use Dust (0.1% concentrate). Feeders (500 mL capacity) were replenished every 24 hours over a continuous 30-day period.

### 3.1. Bee Tagging

We trained forager bees to locate artificial feeders by gradually moving feeders containing 50% sucrose solution from hive entrances to a final distance of 10 meters. Once consistent foraging patterns were established, we captured departing foragers at hive entrances and marked them with 5 mm diameter circular tags, inspired by a modified BeesBook protocol (Wario, Wild, Rojas and Landgraf, 2017) (Figure 1). Each tag had two functional components. The outer ring displayed an 8-sector binary code encoding individual bee identity, supporting up to 256 unique IDs per colony. The inner semicircle orientation marker, with its black half facing the bee's head, enabled automated detection of entry versus exit movements. The binary-coded design offers benefits such as rotation invariance and motion blur tolerance that improve detection performance compared to numeric tags or barcodes. Tags were affixed to the thoracic dorsum using cyanoacrylate adhesive.

### 3.2. Data Acquisition

#### 3.2.1. Behavioral and Acoustic Recording

We deployed an automated monitoring system to continuously record foraging behavior and hive acoustics over 30 days (Figure 2). Video and audio streams were captured by Raspberry Pi 4B units and transmitted to processing computers for offline analysis.

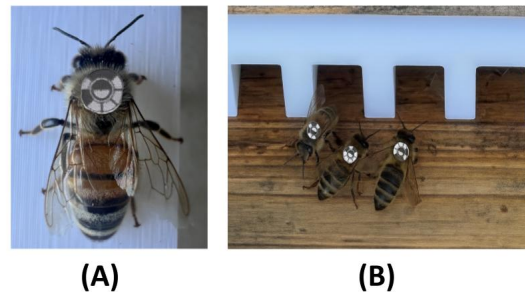


**Figure 1:** Bee tagging and monitoring. (A) Individual bee with binary-coded identification tag attached to thoracic dorsum. (B) Tagged workers at custom-designed hive entrance for automated tracking.

The system operated autonomously using 20 W solar panels with lithium-ion battery backup.

We positioned an Arducam IMX519 camera approximately 40 cm above hive entrances to capture bee traffic without disturbing colony activity. The cameras recorded at 720p resolution and 60 frames per second using back-illuminated sensors with 1.22  $\mu\text{m}$  pixel pitch and f/1.75 autofocus lenses. Custom entrance tunnels channeled bee movement to maximize tag visibility in the camera field of view.

We placed PoP Voice omnidirectional microphones inside hive entrances to record internal colony acoustics. The microphones featured 30 dB sensitivity and a 20 Hz to 20 kHz frequency response, capturing wingbeat frequencies and collective hive sounds. Built-in noise cancellation reduced ambient environmental interference.

The automated tracking system recorded entrance and exit timestamps for each tagged bee, resulting in a dataset of 34,282 foraging trips from 433 individuals across 6 colonies (Table 1). In parallel, the acoustic dataset consisted of 7,200 thirty-second audio segments.

#### 3.2.2. Weather Monitoring

An AcuRite Pro weather station positioned within 10 meters of the hives measured temperature, relative humidity, wind speed, and precipitation at hourly intervals. The station transmitted data to a computer via USB connection through the PC Connect software interface.



**Figure 2:** Automated bee monitoring system components. (A) Camera positioned above hive entrance for image capture, (B) Raspberry Pi for data transfer and system control, (C) Solar panel for a sustainable power supply, and (D) Microphone for bee sound recording.

**Table 1**

Summary of tagged bees and recorded trips by treatment group

Group	Concentration	Bees	Trips
Control	–	148	13,129
Imidacloprid	10 ppb	145	9,875
Bifenthrin	10 ppb	140	11,278
<b>Total</b>	–	<b>433</b>	<b>34,282</b>

### 3.3. Data Annotation for Bee Identification

We used Label Studio to annotate individual bees from sampled video frames (Figure 3). For each frame, we drew bounding boxes (BBox) around bee bodies and wings, generating label files in YOLO format containing object ID, BBox X-axis center, Y-axis center, width, and height. Each bee in multi-bee frames received a separate annotation line.

To ensure annotation quality, we excluded frames where bees showed less than 50% body visibility or were excessively blurred. Two annotators independently verified a random subset of annotations to ensure consistency. After detecting bees with YOLO, we applied the same annotation pipeline to identify and label individual bee tags.

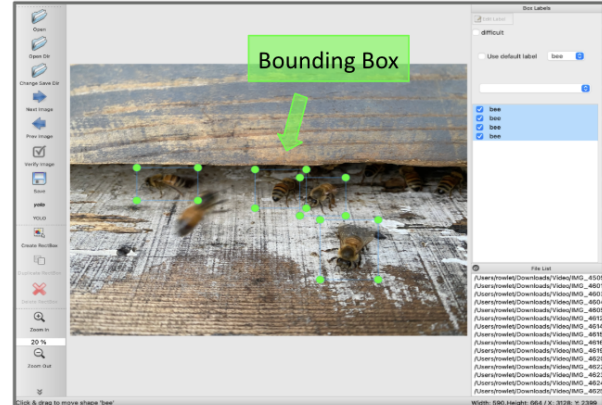


**Figure 3:** Bee detection sample annotation in the Label Studio.

### 3.4. Feature Engineering

Predicting pesticide exposure from behavior requires features mechanistically linked to pesticide effects while remaining robust to natural variation. We designed features from foraging behavior and hive acoustics that capture pesticide-induced disruptions validated in neurobiology studies, while incorporating environmental context to distinguish contamination from weather-driven changes.

### 3.4.1. Behavioral Features from Foraging Activity

Sublethal pesticide exposure disrupts honey bee foraging through three neural pathways: cholinergic impairment affects motor coordination, navigational memory degradation disrupts spatial processing, and metabolic stress alters energy allocation (Crall and Raine, 2023; Bullinger, Greggers and Menzel, 2023; Kuo, Lu, Lin, Lin and Wu, 2023). We extracted eight daily metrics from the beehive entry and exit timestamps, including activity intensity (trip count, total flight duration, in-hive duration), foraging efficiency (average trip duration, trip rate as trips per active hour), and circadian regulation (first departure hour, last return hour, trip window from first departure to final return).

This design enables detection across pesticide classes with different modes of action: neonicotinoids primarily disrupt circadian timing, organophosphates impair motor coordination, and pyrethroids affect both (Tasman, Rands and Hodge, 2020; Stuligross, Melone, Wang and Williams, 2023).

### 3.4.2. Acoustic Features from Hive Sounds

Hive acoustics reveal collective stress responses invisible to entrance monitoring. We sampled audio at 16 kHz, capturing bee wingbeat frequencies from 200 to 300 Hz fundamentals through their 1 kHz harmonics. From raw audio streams, we extracted 13 Mel-frequency cepstral coefficients (MFCC) using 25 ms Hamming windows with 10 ms overlap. MFCCs capture spectral patterns in wingbeat frequencies and collective buzzing while reducing dimensionality by three orders of magnitude compared to raw spectrograms, enabling efficient transformer processing.

### 3.4.3. Environmental Features from Weather Monitoring

A fundamental challenge in field monitoring is distinguishing pesticide effects from weather-driven behavioral changes. We recorded temperature, relative humidity, wind speed, and precipitation at hourly intervals and aggregated them to daily means, matching the temporal resolution of behavioral and acoustic features. We used only mean values to

avoid multicollinearity from including minimum and maximum statistics. Weather features enable the model to learn context-dependent patterns: reduced foraging activity during adverse weather reflects normal behavior, whereas unexplained reductions on favorable days signal potential pesticide exposure.

## 4. Methods

### 4.1. Bee Tracking and Identification

We employ a two-stage YOLOv8 pipeline for bee localization and tag identification. The first stage detects individual bees in video frames using a model trained on 1,524 annotated frames spanning diverse lighting conditions and colony activity levels. The second stage processes detected bee regions to identify binary tags, trained on 1,856 cropped bee images. Both models use data augmentation, including geometric transformations (rotation  $\pm 15^\circ$ , scaling 0.8–1.2 $\times$ ), photometric adjustments (brightness  $\pm 20\%$ , contrast  $\pm 15\%$ , saturation  $\pm 10\%$ ), and spatial augmentations (horizontal and vertical flipping) to ensure robust performance across diverse field conditions.

Detected tags are subsequently processed through an EfficientNet-B0 network with dual-task heads for simultaneous bee ID classification and movement direction detection. For each bee crossing the hive entrance boundary, the system records individual ID, direction, and timestamp. Consecutive detections within 2-second windows for the same bee are merged to eliminate duplicates.

### 4.2. Pesticide Exposure Prediction

#### 4.2.1. Problem Formulation

We formulate pesticide exposure detection as a sequential classification problem over multimodal data. We collect bee behavioral features  $\mathbf{x}_{\text{foraging},t}^{(i)} \in \mathbb{R}^8$ , acoustic features  $\mathbf{x}_{\text{audio},t} \in \mathbb{R}^{13}$ , and weather conditions  $\mathbf{x}_{\text{weather},t} \in \mathbb{R}^4$  at each day  $t$  over the total observation period of  $T_i$  days. Unlike fixed-window approaches, the sequence length  $T_i$  varies across bees due to natural mortality. Our objective is to predict pesticide exposure  $y^{(i)} \in \{0, 1\}$  using observations up to detection time  $t \leq T_i$ .

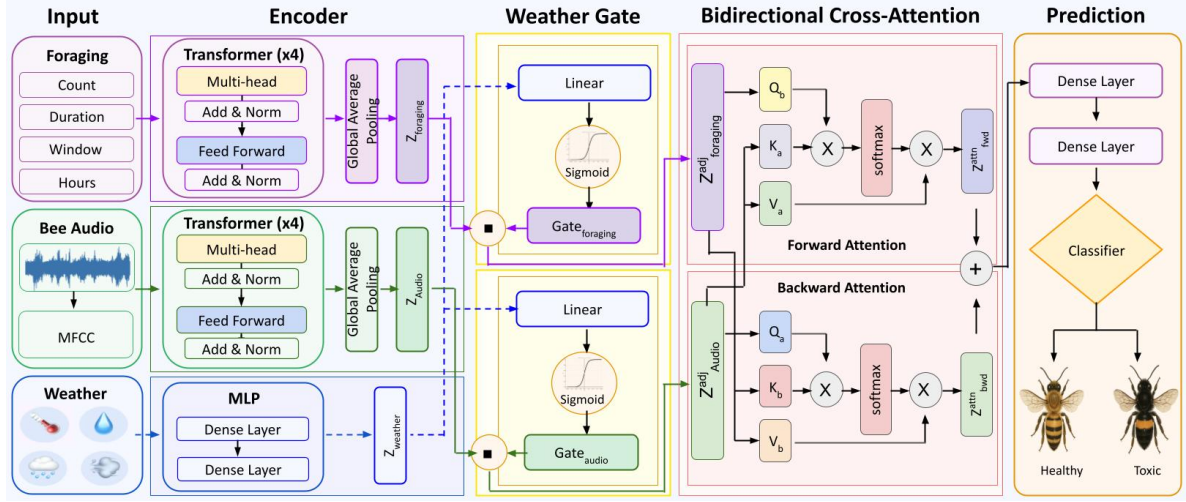


**Figure 4:** WCM-Net Architecture for Pesticide Exposure Detection. The framework processes three data streams: foraging behavior, hive acoustics, and weather conditions. (1) Transformer encoders capture long-range temporal dependencies in foraging behavior and hive acoustics, (2) weather-contextualized gating adjusts features based on environmental context through learned modality-specific gates, and (3) bidirectional cross-modal attention fuses complementary signals. A two-layer classifier produces binary exposure predictions.

### 4.3. WCM-Net Model Architecture

We developed the Weather-contextualized Multimodal Network (WCM-Net) that integrates individual bee foraging behavior and acoustics to detect environmental pesticide contamination while controlling for weather factors (Figure 4). The core contribution is weather-contextualized gating that learns to adjust each modality based on environmental context before cross-modal integration.

#### 4.3.1. Modality-Specific Encoders

**Behavior Encoder.** Pesticide effects accumulate over days, requiring models that preserve long-range dependencies. We use a 4-layer Transformer encoder with 8 attention heads and 256-dimensional hidden states with sinusoidal positional encoding. We choose Transformers over LSTMs because self-attention models dependencies across all time steps without vanishing gradients, connecting day 1 exposure to day 30 impairment directly.

After encoding individual sequences, we aggregate per-bee embeddings via learned attention pooling to obtain bee foraging embeddings  $\mathbf{z}_{\text{foraging}} \in \mathbb{R}^{256}$ . This automatically weights experienced foragers more

heavily with accumulated exposure than newly emerged bees with minimal foraging.

**Acoustic Encoder.** Hive acoustics capture colony-level stress responses invisible to entrance monitoring, such as agitated buzzing or disrupted wingbeat coordination. Daily MFCC sequences from 30-second audio clips are processed by an identical 4-layer Transformer with 8 heads and 256 hidden units. We apply Transformers directly to MFCCs rather than adding convolutional layers because MFCCs already encode frequency structure through discrete cosine transformation, making additional spectral preprocessing redundant. The self-attention mechanism learns which temporal segments are diagnostic. Global average pooling produces the hive acoustic embedding  $\mathbf{z}_{\text{audio}} \in \mathbb{R}^{256}$ .

**Weather Encoder.** Weather provides contextual information for interpreting behavior and acoustics rather than a diagnostic signal, so we intentionally use a lightweight two-layer multilayer perceptron (MLP) to produce the weather embedding  $\mathbf{z}_{\text{weather}} \in \mathbb{R}^{64}$ . Over-parameterizing this branch would misallocate model capacity away from learning pesticide patterns, which are the actual prediction target.

### 4.3.2. Weather-contextualized Gating

Simple concatenation of multimodal embeddings forces the classifier to implicitly separate weather from pesticide effects. Manual normalization approaches, such as z-score standardization, apply uniform transformations across all conditions and cannot capture nonlinear, context-dependent relationships between weather and behavior. We introduce explicit weather-dependent gating mechanisms that modulate behavior and acoustic features based on weather conditions before cross-modal fusion, enabling the model to learn modality-specific weather adjustments automatically:

$$\mathbf{g}_m = \sigma(\mathbf{W}_{g_m} \mathbf{z}_{\text{weather}} + \mathbf{b}_{g_m}) \quad (1)$$

where  $m \in \{\text{foraging, audio}\}$ ,  $\sigma$  is the sigmoid function,  $\mathbf{W}_{g_m} \in \mathbb{R}^{256 \times 64}$  is a learned weight matrix,  $\mathbf{b}_{g_m} \in \mathbb{R}^{256}$  is a bias vector, and  $\mathbf{z}_{\text{weather}} \in \mathbb{R}^{64}$  is the weather embedding. For each modality  $m$ , this produces 256 gate values in  $[0,1]$  applied via element-wise multiplication:

$$\mathbf{z}_m^{\text{adj}} = \mathbf{z}_m \odot \mathbf{g}_m \quad (2)$$

where  $\odot$  denotes element-wise multiplication and  $\mathbf{z}_m^{\text{adj}} \in \mathbb{R}^{256}$  is the weather-adjusted embedding.

Gate values  $\mathbf{g}_m$  near 1.0 preserve weather-invariant features (e.g., navigation errors and flight duration variance), while values near 0.0 suppress weather-dependent features (e.g., reduced flight counts on extreme temperature days). Separate gates for behavior and acoustics accommodate their asymmetric weather dependencies: temperature reduces flight activity by up to 40%, but shifts wingbeat frequency by only 2 Hz/°C (Kenna, Pawar and Gill, 2021; Saha et al., 2024).

### 4.3.3. Bidirectional Cross-Modal Attention

Weather-adjusted embeddings are fused via bidirectional attention to model mutual dependencies between foraging disruptions and acoustic stress.

**Forward attention** uses behavior as the query and audio as key/value to identify which acoustic features are most relevant given the observed behavioral patterns:

$$\mathbf{z}_{\text{fwd}}^{\text{attn}} = \text{Attention}(\mathbf{W}_Q \mathbf{z}_{\text{foraging}}^{\text{adj}}, \mathbf{W}_K \mathbf{z}_{\text{audio}}^{\text{adj}}, \mathbf{W}_V \mathbf{z}_{\text{audio}}^{\text{adj}}) \quad (3)$$

where  $\mathbf{W}_Q, \mathbf{W}_K, \mathbf{W}_V \in \mathbb{R}^{256 \times 256}$  are learned projection matrices and  $\mathbf{z}_{\text{fwd}}^{\text{adj}} \in \mathbb{R}^{256}$ .

**Backward attention** reverses roles to identify behavioral patterns correlating with acoustic signals.

$$\mathbf{z}_{\text{bwd}}^{\text{attn}} = \text{Attention}(\mathbf{W}_{Q'} \mathbf{z}_{\text{audio}}^{\text{adj}}, \mathbf{W}_{K'} \mathbf{z}_{\text{foraging}}^{\text{adj}}, \mathbf{W}_{V'} \mathbf{z}_{\text{foraging}}^{\text{adj}}) \quad (4)$$

where  $\mathbf{W}_{Q'}, \mathbf{W}_{K'}, \mathbf{W}_{V'} \in \mathbb{R}^{256 \times 256}$  are learned projection matrices and  $\mathbf{z}_{\text{bwd}}^{\text{attn}} \in \mathbb{R}^{256}$ .

The concatenated output  $\mathbf{z}_{\text{fused}} \in \mathbb{R}^{512}$  preserves complementary information from both perspectives ( $\mathbf{z}_{\text{fwd}}^{\text{attn}}$  and  $\mathbf{z}_{\text{bwd}}^{\text{attn}}$ ) through a linear projection.

### 4.3.4. Classification

The fused representation  $\mathbf{z}_{\text{fused}}$  passes through two dense layers with ReLU and dropout, then a sigmoid output produces  $p \in [0, 1]$ . We optimize binary cross-entropy loss with L2 regularization using AdamW optimizer with a learning rate  $10^{-4}$ , cosine learning rate decay, and early stopping with patience of 20 epochs to prevent overfitting.

## 4.4. Model Interpretability

We implemented two complementary interpretability analyses to understand model decisions: temporal analysis revealing when these patterns become important during pesticide exposure progression, and feature-level analysis identifying which behavioral patterns are most discriminative. Together, these analyses provide insights into both the temporal dynamics of behavioral deterioration and the biological mechanisms of pesticide effects.

#### 4.4.1. Temporal Feature Attribution Analysis

To reveal the temporal evolution of feature timestamp throughout the exposure period, we computed time-resolved gradient-based attributions. For each feature  $x_i$  at time step  $t$ , we calculated the temporal attribution score as:

$$A_{i,t} = \frac{1}{N} \sum_{n=1}^N \left| \frac{\partial \hat{y}_n}{\partial x_{i,t}^{(n)}} \right| \quad (5)$$

where  $\hat{y}_n$  represents the model prediction for sample  $n$ , and  $x_{i,t}^{(n)}$  denotes the value of feature  $i$  at time  $t$  for sample  $n$ . Feature importance scores are normalized from 0 to 1, where 1 represents maximum discriminative power and values below 0.5 indicate limited utility for classification.

#### 4.4.2. Feature Importance Analysis

To identify the most discriminative behavioral features for pesticide exposure, we aggregated gradient-based attribution scores across all time steps:

$$I_i = \sum_{t=1}^T A_{i,t} \quad (6)$$

where  $I_i$  represents the total importance of feature  $i$  across all time steps, and  $A_{i,t}$  denotes the attribution score for feature  $i$  at time  $t$ . The aggregated feature importance scores were then normalized to sum to one across all features.

## 5. Results

### 5.1. Experiment Setup

Bees were randomly assigned to training (60%), validation (20%), and testing (20%) datasets. We primarily assessed model performance using area under the curve (AUC), a threshold-independent metric well-suited for biological applications where decision thresholds may vary (Barendregt, Gold, Josić and Kilpatrick, 2022). Secondary metrics included precision, recall, and F1-score. Each experiment was repeated across 30 random seeds to ensure statistical reliability, with results summarized as mean  $\pm$  standard deviation.

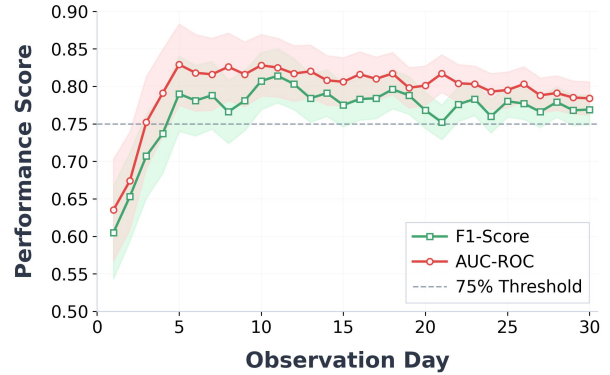


**Figure 5:** WCM-Net performance over observation period. AUC and F1-score demonstrate progressive improvement, with reliable detection (AUC  $> 0.75$ ) achieved by day 3 and peak performance reaching 0.829 AUC by day 5. Shaded areas represent 95% confidence intervals.

Model training was performed on NVIDIA Tesla V100 GPUs equipped with 32 GB of RAM.

### 5.2. Bee Detection and Tracking Accuracy

The bee detection and tracking pipeline comprises three sequential detection stages. First, YOLOv8 bee detection demonstrated 94.8% precision, 95.9% recall, and 98.6% mAP@50. Second, the specialized YOLOv8 tag detection network achieved 82.8% precision, 83.9% recall, and 85.6% mAP@50. Third, the EfficientNet-B0 dual-head classifier achieved 81.1% accuracy for bee ID classification and 82.9% accuracy for directional movement detection.

### 5.3. WCM-Net Performance Evaluation

#### 5.3.1. Overall Classification Results

We assessed WCM-Net's performance to detect pesticide exposure over a 30-day observation period (Figure 5). During the early phase (days 1–5), AUC increased from 0.635 to 0.829 with a mean of  $0.736 \pm 0.061$ , while F1-score improved from 0.605 to 0.790 with a mean of  $0.698 \pm 0.056$ . The model achieved reliable detection (AUC  $> 0.75$ ) as early as day 3.

After day 5, WCM-Net maintained robust predictive performance with AUC values ranging from 0.784 to 0.828 and averaging  $0.807 \pm 0.031$ , while F1-scores ranged from 0.752 to 0.814 with a mean of  $0.781 \pm 0.029$ . Overall, the model attained a mean AUC of  $0.805 \pm 0.036$  across all 30 days, with

**Table 2**WCM-Net Ablation Study Results. <sup>†</sup> Day represents first observation when AUC > 0.75.

Model Variant	Early AUC (1–5d)	Mean AUC	Peak AUC	Day <sup>†</sup>	ΔAUC
<b>WCM-Net (Full)</b>	<b>0.736±0.061</b>	<b>0.805±0.036</b>	<b>0.829</b>	<b>3</b>	–
w/o Cross Attention	0.692±0.065	0.749±0.041	0.786	4	-0.056
w/o Weather Gating	0.680±0.066	0.727±0.042	0.774	5	-0.078
w/o Weather	0.657±0.066	0.713±0.040	0.754	7	-0.092
Foraging Only	0.647±0.068	0.702±0.043	0.743	9	-0.103
Audio Only	0.623±0.070	0.682±0.045	0.714	11	-0.123

peak performance of 0.829 AUC reached on day 5. Confidence intervals progressively narrowed from  $\pm 0.068$  to  $\pm 0.022$  for AUC and from  $\pm 0.072$  to  $\pm 0.024$  for F1-score between days 1 and 30.

### 5.3.2. Ablation Study

To quantify the contribution of each architectural component, we conducted systematic ablation experiments (Table 2). Single-modality models exhibited substantial performance degradation. The audio-only model yielded the weakest results, achieving a mean AUC of 0.682 ( $\Delta$ AUC = -0.123) and a peak AUC of 0.714, with reliable detection delayed until day 11. The foraging-only variant performed moderately better with a mean AUC of 0.702 ( $\Delta$ AUC = -0.103) and a peak AUC of 0.743, reaching the detection threshold by day 9, representing a 0.020 AUC improvement over the audio-only approach.

Weather contextualization proved essential for accurate detection. Complete removal of weather features decreased mean AUC to 0.713 and peak AUC = 0.754, postponing threshold attainment to day 9. The weather gating mechanism alone accounted for 0.078 AUC; its removal resulted in mean AUC of 0.727 and peak AUC of 0.774, delaying detection to day 7. Similarly, the cross-attention mechanism contributed 0.056 AUC, as evidenced by the w/o Cross Attention variant achieving mean AUC of 0.749 and peak AUC of 0.786, also with day 7 threshold detection.

The importance of multimodal integration was particularly evident during early detection phases (days 1–5). Early AUC values declined progressively from  $0.736\pm0.061$  for the full model to  $0.692\pm0.065$

(w/o Cross Attention),  $0.680\pm0.066$  (w/o Weather Gating),  $0.657\pm0.066$  (w/o Weather),  $0.647\pm0.068$  (Foraging Only), and  $0.623\pm0.070$  (Audio Only). This consistent degradation pattern underscores the synergistic value of combining multiple data modalities with sophisticated fusion mechanisms for early pesticide exposure detection.

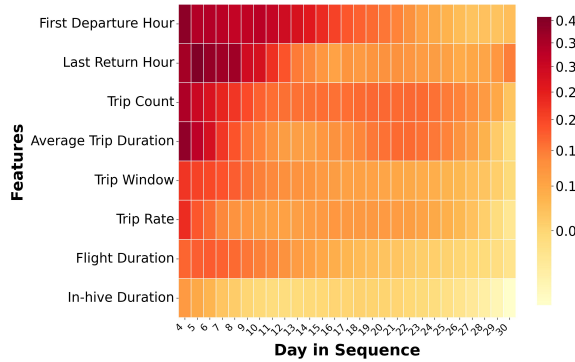
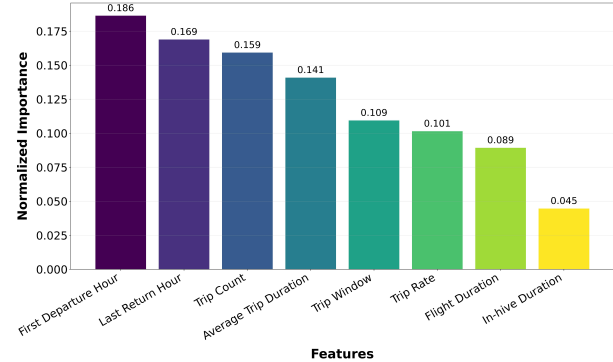
### 5.3.3. Baseline Comparison

We benchmarked WCM-Net against four conventional machine learning approaches over the 30-day period (Table 3). WCM-Net substantially outperformed all baselines across every metric, demonstrating early AUC of  $0.736\pm0.061$ , mean AUC of  $0.805\pm0.036$ , and peak AUC of 0.829, while achieving the detection threshold earliest at day 3.

Among the baseline models, GRU displayed the most competitive performance, attaining a mean AUC of 0.737 ( $\Delta$ AUC = -0.068) and peak AUC of 0.775, with threshold crossing at day 5. SVM performed moderately with a mean AUC of 0.702 ( $\Delta$ AUC = -0.103) and peak AUC of 0.755, reaching the threshold at day 8. Random Forest showed considerable degradation with a mean AUC of 0.659 ( $\Delta$ AUC = -0.146) and peak AUC of 0.708, achieving reliable detection only by day 11. Logistic Regression exhibited the weakest performance, recording a mean AUC of 0.612 ( $\Delta$ AUC = -0.193) and peak AUC of 0.662, never exceeding the 0.75 detection threshold throughout the entire 30-day evaluation period, with peak performance occurring at day 14.

**Table 3**Baseline Model Comparison. <sup>†</sup> Day represents first observation when AUC > 0.75.

Model	Early AUC (1–5d)	Mean AUC	Peak AUC	Day <sup>†</sup>	ΔAUC
WCM-Net	<b>0.736±0.061</b>	<b>0.805±0.036</b>	<b>0.829</b>	<b>3</b>	–
GRU	0.687±0.065	0.737±0.041	0.775	5	-0.068
SVM	0.650±0.068	0.702±0.043	0.755	8	-0.103
Random Forest	0.605±0.072	0.659±0.044	0.708	11	-0.146
Logistic Regression	0.560±0.075	0.612±0.046	0.662	14	-0.193

**Figure 6:** Temporal attribution heatmap across observation days. Feature importance is highest in early days and declines over time.**Figure 7:** Feature importance scores for imidacloprid exposure detection. First departure hour and average trip duration are the most predictive behavioral indicators.

## 5.4. Interpretability Analysis

### 5.4.1. Feature Importance Temporal Dynamics

Temporal feature attribution analysis reveals the dynamic importance of behavioral features across the 30-day observation period (Figure 6). Feature importance peaked during the early learning phase (days 1–5) and progressively declined. Temporal features (first departure hour, last return hour) demonstrated the strongest discriminative power in early detection. Trip-level metrics (trip count, average trip duration, trip rate) maintained moderate to elevated importance through day 6, then gradually diminished. Window-based features (trip window, flight duration) showed comparable patterns with slightly lower peak importance during days 1–4. Consistent with the overall feature ranking, in-hive duration exhibited the lowest temporal importance across all observation days.

### 5.4.2. Feature Importance Analysis Results

Feature importance analysis showed distinct contributions of foraging and acoustic features to

pesticide exposure prediction (Figure 7). Temporal features dominated predictive power, with first departure hour achieving the highest importance score (0.186), followed closely by last return hour (0.169). Trip-level metrics demonstrated substantial contributions: trip count (0.158), average trip duration (0.141), trip window (0.109), trip rate (0.101), and flight duration (0.089). Notably, in-hive duration exhibited the lowest importance score (0.045), suggesting that foraging patterns provide more discriminative signals than nest residency time for detecting pesticide exposure.

## 6. Discussion

Our findings demonstrate that WCM-Net enables reliable early detection of pesticide exposure in honey bees, achieving an AUC of  $0.736 \pm 0.061$  within the first three days and sustaining strong performance across the full monitoring window (mean AUC  $0.805 \pm 0.036$ ). This capacity to identify exposure at an early stage is

critical for environmental surveillance, as honey bees act as sentinel organisms whose behavioral disruptions provide early warning signals of contamination. The model's strength lies in its integration of foraging behavior, acoustic signatures, and weather contextualization—complementary data streams that together capture the multifaceted physiological disturbances caused by pesticide exposure. In contrast to prior methods that rely on single modalities or manual observations, WCM-Net delivers automated, continuous, and objective monitoring at the scale required for systematic ecosystem assessment.

The ablation analysis shows that each architectural component plays a distinct role, with performance driven by their combined effect. Removing weather features reduced mean AUC by 0.092, while excluding the gating mechanism alone lowered it by 0.078, highlighting the importance of distinguishing pesticide-induced behavior from normal weather-driven variation. Without these mechanisms, the model misclassified weather responses as exposure signals, leading to false positives or false negatives. Cross-modal attention provided an additional gain of 0.056 AUC by learning relationships between foraging and acoustic changes, such as disrupted foraging rhythms paired with stress-induced acoustic shifts (Klein, Cabirol, Devaud, Barron and Lihoreau, 2017). Single-modality approaches averaging 0.682–0.702 AUC underperformed considerably compared to the full model at 0.805 AUC. These results confirm that pesticide exposure manifests across multiple behavioral dimensions, consistent with biological evidence that pesticide impairs both nicotinic acetylcholine receptor function that affects flight coordination and colony-level communication (Chen, Tzeng and Yang, 2021).

Baseline comparisons further underline the advantage of deep learning for temporal behavioral analysis. While the GRU baseline captured sequential dependencies reasonably well (mean AUC 0.737), its lack of explicit cross-modal modeling limited sensitivity (AUC = -0.068). Traditional machine learning methods performed progressively worse: SVM reached only 0.702 (AUC = -0.103), Random Forest 0.659 (AUC

= -0.146), and Logistic Regression 0.612 (AUC = -0.193). Importantly, these models crossed the 0.75 AUC threshold much later (days 8–14) than WCM-Net (day 3), diminishing their practical utility since sublethal damage accumulates rapidly during initial exposures. The progressive narrowing of confidence intervals, from  $\pm 0.068$  on day 1 to  $\pm 0.022$  on day 30, suggests that WCM-Net develops increasingly stable representations as exposure signatures grow more distinct over time.

From an applied perspective, achieving reliable detection at 0.75 AUC by day 3 has significant implications. For beekeepers, early detection supports intervention strategies such as hive relocation, supplemental feeding, or treatment application before worker bee populations decline. For regulatory agencies and environmental managers, it provides rapid feedback on pesticide contamination, enabling timely responses such as issuing public health advisories, conducting targeted soil and water sampling in affected areas, implementing temporary restrictions on pesticide applications, or initiating investigations into potential drift events. This early warning capacity is particularly valuable for monitoring compliance with pesticide-free zones near sensitive habitats and for detecting unauthorized or excessive applications before ecological damage cascades through pollinator networks.

Interpretability analysis clarifies which features most strongly signal exposure. Temporal rhythm disruptions dominated, with first departure hour (0.186) and last return hour (0.169) emerging as the leading predictors, consistent with known effects of pesticides on circadian regulation and spatial memory (Honatel, Arbo, Leal, da Silva Júnior, Garcia and Arbo, 2024). Trip-level indicators including trip count, average trip duration, and trip rate contributed moderately (0.101–0.158), reflecting reduced foraging efficiency as neurotoxic effects accumulated. As shown in Figure 6, these signals were strongest in the first five days, after which their discriminability declined, suggesting acute disruption followed by partial behavioral adjustment (Herman,

2013). In contrast, in-hive duration carried minimal predictive value (0.045), indicating that hive residency patterns remain largely stable even as external foraging deteriorates. These patterns align with neurotoxicological literature showing that pesticides preferentially disrupt higher-order tasks such as navigation and temporal learning while leaving basic motor functions relatively intact during sublethal exposure (Fischer, Müller, Spatz, Greggers, Grünwald and Menzel, 2014; Williamson, Willis and Wright, 2014).

Despite its promise, several limitations remain. This study focused solely on imidacloprid at field-realistic concentrations under controlled feeder-based conditions. Broader validation across other neonicotinoids, organophosphates, and pyrethroids is needed, as each class operates through distinct neurotoxic mechanisms and may leave different behavioral signatures. The dataset including 433 bees across six colonies offers a modest sample, and sensitivity may vary by geography, subspecies, or season. Furthermore, we addressed only binary classification (exposed vs. control), whereas real-world monitoring would benefit from identifying pesticide class and concentration. Future work should therefore expand the dataset across diverse compounds and field contexts, develop models for concentration-level prediction, and pursue edge-deployable architectures with robust noise handling to enable practical real-time use in beekeeping and environmental management.

## 7. Applications

The WCM-Net framework is deployed through a mobile application that translates complex temporal behavioral analyses into clear, actionable insights for commercial beekeepers, environmental regulators, and agricultural researchers. The platform delivers automated pesticide exposure detection (Figure 8A), feature-level analyses that highlight specific behavioral disruptions (Figure 8B), and longitudinal tracking of colony health (Figure 8C). Users can upload data for immediate evaluation and receive automated alerts when contamination is detected.

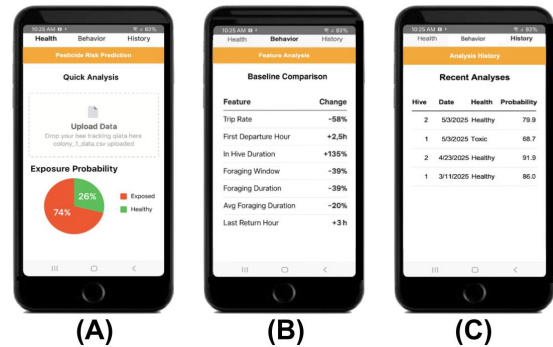


**Figure 8:** WCM-Net mobile application interface. (A) Data upload and pesticide exposure assessment, (B) Behavioral deviation analysis from baseline, and (C) Historical exposure records.

## 8. Conclusion

This study presents WCM-Net, a multimodal deep learning framework that integrates foraging behavior, colony acoustics, and weather context to enable early and accurate detection of pesticide exposure in honey bees. The model achieved reliable detection within three days ( $AUC = 0.736 \pm 0.061$ ) and sustained strong performance over the 30-day period (mean  $AUC = 0.805 \pm 0.036$ , peak  $AUC = 0.829$ ). Ablation experiments confirmed the complementary contributions of the Transformer encoder, weather-conditioned gating, and cross-modal attention in separating pesticide-induced disruptions from normal environmental variation, while feature attribution analysis identified temporal rhythm disruption as the most sensitive early behavioral signal of pesticide exposure.

Compared with traditional machine learning approaches, WCM-Net delivers substantially earlier and more reliable detection while offering interpretable insights into the underlying behavioral mechanisms. This early detection capability serves dual purposes: enabling beekeepers to protect colonies through timely interventions such as hive relocation, and providing regulatory agencies with rapid evidence for compliance monitoring, contamination source identification, and enforcement actions. These capabilities establish a foundation for deploying honey bees as sentinel organisms in precision agriculture

and ecosystem health monitoring. Future directions include expanding the framework to multi-pesticide detection, extending prediction to concentration levels, and developing edge-computable implementations that support real-time field deployment across agricultural landscapes.

## References

Ahsan, Z., Wu, Z., Lin, Z., Ji, T., Wang, K., 2025. The sublethal effects of neonicotinoids on honeybees. *Biology* 14, 1076. doi:10.3390/biology14081076.

Barascou, L., Requier, F., Sené, D., Crauser, D., Le Conte, Y., Alaux, C., 2022. Delayed effects of a single dose of a neurotoxic pesticide (sulfoxaflor) on honeybee foraging activity. *Science of The Total Environment* 805, 150351. doi:10.1016/j.scitotenv.2021.150351.

Barendregt, N.W., Gold, J.I., Josić, K., Kilpatrick, Z.P., 2022. Normative decision rules in changing environments. *eLife* 11, e79824. doi:10.7554/eLife.79824.

Boenisch, F., Wild, B., Dormagen, D., et al., 2021. Automated video monitoring of unmarked and marked honey bees. *Frontiers in Computer Science* 3, 769338.

Bullinger, E., Greggers, U., Menzel, R., 2023. Generalization of navigation memory in honeybees. *Frontiers in Behavioral Neuroscience* 17, 1070957. doi:10.3389/fnbeh.2023.1070957.

Cabirol, A., Haase, A., 2019. The neurophysiological bases of the impact of neonicotinoid pesticides on the behaviour of honeybees. *Insects* 10, 344. doi:10.3390/insects10100344.

Chen, Y.R., Tzeng, D.T., Yang, E.C., 2021. Chronic effects of imidacloprid on honey bee worker development—molecular pathway perspectives. *International Journal of Molecular Sciences* 22, 11835.

Colin, T., Meikle, W.G., Wu, X., Barron, A.B., 2019. Traces of a neonicotinoid induce precocious foraging and reduce foraging performance in honey bees. *Environmental Science & Technology* 53, 8252–8261.

Colin, T., Warren, R.J., Quarrell, S.R., Allen, G.R., Barron, A.B., 2022. Evaluating the foraging performance of individual honey bees in different environments with automated field rfid systems. *Ecosphere* 13, e4088. doi:10.1002/ecs2.4088.

Crall, J.D., Raine, N.E., 2023. How do neonicotinoids affect social bees? linking proximate mechanisms to ecological impacts, in: *Advances in Insect Physiology*. Academic Press. volume 64, pp. 191–253.

Delaplane, K.S., Van Der Steen, J., Guzman-Novoa, E., 2013. Standard methods for estimating strength parameters of apis mellifera colonies. *Journal of Apicultural Research* 52, 1–12. doi:10.3896/IBRA.1.52.1.03.

Di, N., Zhu, C., Hu, Z., Sharif, M.Z., Yu, B., Liu, F., 2025. Honeybee colony soundscapes: Decoding distance-based cues and environmental stressors. *Ecotoxicology and Environmental Safety* 297, 118241.

Dormagen, D., Wild, B., 2021. Beesbook: The social network. URL: <https://communities.springernature.com/posts/beesbook-the-social-network>. accessed: YYYY-MM-DD.

Fischer, J., Müller, T., Spatz, A.K., Greggers, U., Grünewald, B., Menzel, R., 2014. Neonicotinoids interfere with specific components of navigation in honeybees. *PLOS ONE* 9, e91364.

Gernat, T., Rao, V., Middendorf, M., et al., 2022. Automated monitoring of behavior reveals bursty interaction patterns and rapid spreading dynamics in honey bee social networks. *Scientific Reports* 12, 9551.

Goerlitz, H.R., 2018. Weather conditions determine attenuation and speed of sound: Environmental limitations for monitoring and analyzing bat echolocation. *Ecology and Evolution* 8, 5090–5100. doi:10.1002/ece3.4098.

Han, Y., Tian, Y., Li, Q., Yao, T., Yao, J., Zhang, Z., Wu, L., 2025. Advances in detection technologies for pesticide residues and heavy metals in rice: A comprehensive review of spectroscopy, chromatography, and biosensors. *Foods* 14, 1070. doi:10.3390/foods14061070.

Herman, J.P., 2013. Neural control of chronic stress adaptation. *Frontiers in Behavioral Neuroscience* 7, 61. doi:10.3389/fnbeh.2013.00061.

Honatel, K.F., Arbo, B.D., Leal, M.B., da Silva Júnior, F.M.R., Garcia, S.C., Arbo, M.D., 2024. Update on the impact of pesticide exposure on memory and learning. *Discover Toxicology* 1, 11.

Jhawar, J., Davidson, J.D., Weidenmüller, A., Wild, B., Dormagen, D.M., Landgraf, T., Smith, M.L., 2023. How honeybees respond to heat stress from the individual to colony level. *Journal of the Royal Society Interface* 20, 20230290. doi:10.1098/rsif.2023.0290.

Kenna, D., Pawar, S., Gill, R.J., 2021. Thermal flight performance reveals impact of warming on bumblebee foraging potential. *Functional Ecology* 35, 2508–2522. doi:10.1111/1365-2435.13895.

Klein, S., Cabirol, A., Devaud, J.M., Barron, A.B., Lihoreau, M., 2017. Why bees are so vulnerable to environmental stressors. *Trends in Ecology & Evolution* 32, 268–278.

Kuo, Y., Lu, Y.H., Lin, Y.H., Lin, Y.C., Wu, Y.L., 2023. Elevated temperature affects energy metabolism and behavior of bumblebees. *Insect Biochemistry and Molecular Biology* 155, 103932. doi:10.1016/j.ibmb.2023.103932.

Mustafa, S., Mohaghegh, M., Ardekani, I., Sarrafzadeh, A., 2025. Leveraging machine learning approaches to decode hive sounds for stress prediction. *IEEE Access* .

Ngo, T.N., Rustia, D.J.A., Yang, E.C., Lin, T.T., 2021. Automated monitoring and analyses of honey bee pollen foraging behavior using a deep learning-based imaging system. *Computers and Electronics in Agriculture* 187, 106239. doi:10.1016/j.compag.2021.106239.

Olawade, D.B., Wada, O.Z., Ige, A.O., Egbewole, B.I., Olojo, A., Oladapo, B.I., 2024. Artificial intelligence in environmental monitoring: Advancements, challenges, and future directions. *Hygiene and Environmental Health Advances* 12, 100114. doi:10.

1016/j.heha.2024.100114.

O'Reilly, A.D., Stanley, D.A., 2023. Non-neonicotinoid pesticides impact bumblebee activity and pollen provisioning. *Journal of Applied Ecology* 60, 1673–1683. doi:10.1111/1365-2664.14444.

Otesbelgue, A., Orth, A.J., Fong, C.D., Fassbinder-Orth, C.A., Blochtein, B., Pereira, M.J.R., 2025. Hidden markov model for acoustic pesticide exposure detection and hive identification in stingless bees. *PLoS One* 20, e0325732.

Papa, G., Pellecchia, M., Capitani, G., Negri, I., 2025. The use of honey bees (*Apis mellifera* L.) to monitor airborne particulate matter and assess health effects on pollinators. *Environmental Science and Pollution Research* 32, 10357–10369. doi:10.1007/s11356-024-34417-8.

Polders, E., Van Haperen, W., Brijs, T., 2018. Behavioural observation studies.

Robb, E.L., Regina, A.C., Baker, M.B., 2017. Organophosphate toxicity. Details incomplete: please add journal, book, or source information for proper citation.

Saha, T., Genoud, A.P., Park, J.H., Thomas, B.P., 2024. Temperature dependency of insect's wingbeat frequencies: An empirical approach to temperature correction. *Insects* 15, 342. URL: <https://www.mdpi.com/2075-4450/15/5/342>, doi:10.3390/insects15050342. published: 10 May 2024.

Sanchez-Bayo, F., Goka, K., 2014. Pesticide residues and bees—a risk assessment. *PLoS One* 9, e94482. doi:10.1371/journal.pone.0094482.

Shen, S., Qi, W., Zeng, J., Li, S., Liu, X., Zhu, X., Cao, S., 2025. Passive sensing for mental health monitoring using machine learning with wearables and smartphones: Scoping review. *Journal of Medical Internet Research* 27, e77066. doi:10.2196/77066.

Smith, M.L., Vorce, S.P., Holler, J.M., Shimomura, E., Magluilo, J., Jacobs, A.J., Huestis, M.A., 2007. Modern instrumental methods in forensic toxicology. *Journal of Analytical Toxicology* 31, 237–253. doi:10.1093/jat/31.5.237.

Soderlund, D.M., 2010. State-dependent modification of voltage-gated sodium channels by pyrethroids. *Pesticide Biochemistry and Physiology* 97, 78–86. doi:10.1016/j.pestbp.2009.06.004.

Stuligross, C., Melone, G.G., Wang, L., Williams, N.M., 2023. Sublethal behavioral impacts of resource limitation and insecticide exposure reinforce negative fitness outcomes for a solitary bee. *Science of The Total Environment* 867, 161392. doi:10.1016/j.scitotenv.2023.161392.

Tasman, K., Rands, S.A., Hodge, J.J., 2020. The neonicotinoid insecticide imidacloprid disrupts bumblebee foraging rhythms and sleep. *iScience* 23, 101827.

Vincze, C., Lelelössy, , Zajácz, E., Mészáros, R., 2024. A review of short-term weather impacts on honey production. *International Journal of Biometeorology* 69, 303–317. URL: <https://link.springer.com/article/10.1007/s00484-024-02824-0>, doi:10.1007/s00484-024-02824-0.

Wario, F., Wild, B., Rojas, R., Landgraf, T., 2017. Automatic detection and decoding of honey bee waggle dances. *PLOS ONE* 12, e0188626. doi:10.1371/journal.pone.0188626.

Wild, B., Sixt, L., Landgraf, T., 2018. Automatic localization and decoding of honeybee markers using deep convolutional neural networks. *arXiv preprint arXiv:1802.04557*.

Williamson, S.M., Willis, S.J., Wright, G.A., 2014. Exposure to neonicotinoids influences the motor function of adult worker honeybees. *Ecotoxicology* 23, 1409–1418.

Woodcock, B.A., Bullock, J.M., Shore, R.F., Heard, M.S., Pereira, M.G., Redhead, J., Pywell, R.F., 2017. Country-specific effects of neonicotinoid pesticides on honey bees and wild bees. *Science* 356, 1393–1395. doi:10.1126/science.aaa1190.

Yu, B., Huang, X., Sharif, M.Z., Di, N., Liu, F., 2025. A citizen science platform to sample beehive sounds for monitoring ansp. *Journal of Environmental Management* 375, 124247.

Yu, B., Huang, X., Sharif, M.Z., Jiang, X., Di, N., Liu, F., 2023. A matter of the beehive sound: Can honey bees alert the pollution out of their hives? *Environmental Science and Pollution Research* 30, 16266–16276.

Zhao, Y., Deng, G., Zhang, L., Di, N., Jiang, X., Li, Z., 2021. Based investigate of beehive sound to detect air pollutants by machine learning. *Ecological Informatics* 61, 101246.